ChemPubSoc Europe

DOI: 10.1002/chem.201501330

CHEMISTRY A European Journal Full Paper

Single-Ion Magnets

Magnetic Relaxation in Single-Electron Single-Ion Cerium(III) Magnets: Insights from Ab Initio Calculations

Saurabh Kumar Singh,[a] Tulika Gupta,[a] Liviu Ungur,*[b] and Gopalan Rajaraman*[a]

Dedicated to Professor Keith S. Murray on the occasion of his 73rd birthday

Abstract: Detailed ab initio calculations were performed on two structurally different cerium(III) single-molecule magnets (SMMs) to probe the origin of magnetic anisotropy and to understand the mechanism of magnetic relaxations. The complexes $[Ce^{III}\{Zn^{II}(L)\}_2(MeOH)]BPh_4$ (**1**) and $[Li(dme)_3][Ce^{III}(cot'')_2]$ (**1**; L = N,N,O,O-tetradentate Schiff base ligand; **2**; DME = dimethoxyethane, COT'' = 1,4-bis(trimethylsilyl)cyclooctatetraenyldianion), which are reported to be zero-field and field-induced SMMs with effective barrier heights of 21.2 and 30 K respectively, were chosen as examples. CASSCF + RASSI/SINGLE_ANISO calculations unequivocally suggest that $m_J|\pm 5/2\rangle$ and $|\pm 1/2\rangle$ are the ground states for complexes **1** and **2**, respectively. The origin of these differences is rooted back to the nature of the ligand field and the symmetry around the cerium(III) ions. Ab initio magnetisation blockade barriers constructed for complexes **1** and **2** expose a contrasting energy-level pattern with significant quantum tunnelling of magnetisation between the ground state Kramers doublet in complex **2**. Calculations performed on several model complexes stress the need for a suitable ligand environment and high symmetry around the cerium(III) ions to obtain a large effective barrier.

Introduction

Single-molecule magnets (SMMs) are a class of compounds that are sought for their intriguing ability to maintain their intrinsic magnetic moment for some time after the applied magnetic field is switched off. Since the discovery of the first molecular magnet, the $Mn_{12}Ac$ cluster,[1] in the 1990s, exploration of this class of compounds has quickly grown into an active research field. SMMs behave as macroscopic magnets due to several peculiarities of their electronic and magnetic structures, which arise from various molecular interactions. Interesting physical phenomena such as slow relaxation of magnetisation and quantum tunnelling of magnetisation (QTM) has also been revealed for this class of compounds. The magnetisation blocking ability may give rise to potential applications in information storage (the idea of one bit per molecule is attractive), magnetic memory, molecular spintronics and quantum computing devices.[2]

The ideal SMMs must have a certain number of low-lying doublet states characterised by a strong uniaxial anisotropy. The low-lying energy spectrum of $Mn_{12}Ac$ arises as a result of negative zero-field splitting (induced by the anisotropy parameter D, which is usually in the order of several cm^{-1}) of the ground spin $S = 10$; the blocking barrier in this compound is given approximately by $|D|S^2$. However, it is not easy to obtain a large spin ground state S and a very large negative D at the same time to achieve large barrier height for reversal of magnetisation. On the other hand, lanthanide ions have received substantial attention since the initial stages of research into molecular magnetism due to their large magnetic moment;[3] large magnetic anisotropy;[4] unquenched orbital angular momentum; deeply seated unpaired 4f electrons, which result in a negligible ligand field effect; and intrinsic optical[5] and magnetic properties.[6] Given the relatively small radius of the 4f shell, it is almost isolated from the environment and is not significantly involved in covalent interactions and chemical bonding. As a result, the orbital moment of the lanthanide remains unquenched in various ligand environments and induces strong spin–orbit coupling effects in the ground *LS* term. The ground spin–orbital manifold, J, in lanthanide complexes plays the role of the total ground spin in $Mn_{12}Ac$, whereas the crystal field (CF) splitting of the ground J term in complexes (usually of several hundreds of cm^{-1}) may be regarded as the anisotropy of the ground spin in $Mn_{12}Ac$. The advantages of lanthanides for molecular magnetism become clear.[7] Because the size of the ground manifold is fixed to the multiplicity of the ground J term $(2J+1)$, by accurately designing the ligand field around the lanthanide ion, we

[a] S. K. Singh, T. Gupta, Prof. Dr. G. Rajaraman
Department of Chemistry, Indian Institute of Technology Bombay
Powai, Mumbai, 400076 (India)
E-mail: rajaraman@chem.iitb.ac.in

[b] Dr. L. Ungur
Division of Quantum and Physical Chemistry
Department of Chemistry, Katholieke Universiteit Leuven
Celestijnenlaan 200F 3001 Heverlee, Leuven (Belgium)
E-mail: liviu.ungur@chem.kuleuven.be

Supporting information for this article is available on the WWW under http://dx.doi.org/10.1002/chem.201501330.

can induce desired CF splitting and magnetic anisotropy of the resulting states.

Although several mono- and polynuclear lanthanide-based SMMs have been reported so far, interest remains constrained to heavier lanthanide ions, such as Dy^{III}, Tb^{III}, Er^{III} and Ho^{III}, because the spin–orbit coupling is very strong and leads to large magnetic anisotropy.[6d,8,9] On the other hand, lighter lanthanide elements are employed in the production of bulk industrial magnets, such as $SmCo_5$ and $Nd_2Fe_{14}B$.[10] Although the spin–orbit interaction is the vital component for magnetic anisotropy, the CF also has a pronounced effect on the design of SMMs. A recent report by Long and Rinehart revealed the importance of the CF environment on fine-tuning the magnetic properties of lanthanides.[8v] The high coercive field observed in $SmCo_5$ was attributed to the prolate shape of the Sm^{III} ion, with the complete equatorial ligand field offering a large magnetic anisotropy. This study suggests that fine-tuning the ligand field can significantly influence the magnetic behaviour of both the heavy and lighter lanthanide elements.[8v] Among the lighter lanthanides, the Ce^{III} ion has attracted attention in recent years and three SMMs based on Ce^{III} have been reported.[11] Because the Ce^{III} ion possess only one unpaired electron ($4f^1$ configuration and $^2F_{5/2}$ as the ground state) and the natural isotopes of Ce^{III} do not possess any nuclear spin, manipulation of the electronic levels is easier compared with other ions and this has implications for the development of devices based on SMMs.[2e]

Theoretical studies are indispensable in the area of lanthanide chemistry and recent advances in post Hartree–Fock multi-configurational ab initio methodology have made accurate quantum chemical calculations on paramagnetic 4f compounds possible.[8e,l,o,r,s,12] The CASSCF + RASSI/SINGLE_ANISO[12h,13] module implemented in the MOLCAS[14] suite has been widely used to probe magnetic anisotropy in lanthanide molecular magnets.[8n,o,12j,k,15] Considering the recent research trend on early lanthanide-based SMMs, to offer explicit understanding of magnetic anisotropy and magnetic relaxation in varied coordination and metallic environments, we have performed detailed ab initio calculations on Ce^{III}-based SMMs for the first time. Calculations have been performed on two Ce^{III} SMMs: $[Ce^{III}\{Zn^{II}(L)\}_2(MeOH)]BPh_4$ (**1**; L = N,N,O,O-tetradentate Schiff base ligand)[16] and $[Li(dme)_3][Ce^{III}(cot'')_2]$ (**2**; COT'' = 1,4-bis(trimethylsilyl)cyclooctatetraenyldianion, DME = dimethoxyethane). In complex **1**, the Ce^{III} ion is sandwiched between two {Zn(L)} moieties and connected to the Zn^{II} ion through two μ-phenoxo oxygen atoms.[11a,b] These deliberately placed diamagnetic Zn^{II} ions are known to enhance the barrier height by increasing the charge on the phenoxo oxygen atoms and also serve the purpose of dilution.[12aa,17] Complex **1** exhibits slow relaxation of magnetisation in zero field and the U_{eff}, estimated by fitting the data to a non-linear Arrhenius equation, yields a barrier height of 21.2 K (14.7 cm^{-1}). In complex **2**, the Ce^{III} ion is sandwiched by two COT'' ligands. These organometallic ligands are robust towards the synthesis of SMMs because they promote strong electron delocalisation and offer stronger metal–ligand interactions. An example of this category is the $[Er(cot)_2]^-$ complex, which exhibits zero-field SMM behaviour and the second-largest blocking temperature (T_B) of 10 K reported for any SMM to date. Complex **2** exhibits slow relaxation of magnetisation in the presence of an applied static direct current (dc) field and the U_{eff} estimated by using the Arrhenius equation is a barrier height of 30 K (20.9 cm^{-1}). By modelling these two complexes, we intend to answer the following intriguing questions: 1) How do basis sets and the nature of the active space influence the low-lying energy levels in Ce^{III} SMMs? 2) What is the origin of magnetic anisotropy and what are the mechanisms by which magnetic relaxation takes place in these complexes? 3) Why is complex **1** a zero-field SMM, whereas **2** requires an applied dc field to observe relaxation? This question is intriguing given the fact that Ce^{III} does not possess any nuclear spin.[18] 4) Which structures/coordination numbers (C.N.s) are best suited to enhance the U_{eff} for the Ce^{III} ion?

Computational Details

Herein, we have performed all post-Hartree–Fock ab initio calculations by using the MOLCAS 7.8 code.[14] Basis sets describing all atoms were taken from the ANO-RCC[19] library available in the MOLCAS package. Because basis sets[12t] have been found to influence the nature of anisotropy in lanthanide-based systems, we have performed our calculations with three different basis sets with the aim of probing the effect of basis sets on the nature of magnetic anisotropy. Furthermore, we have also varied the active space in Ce^{III} to observe its impact on the anisotropy and relaxation pathway for reorientation of magnetisation. We have performed calculations with three different basis sets: BS1 (931 basis functions), BS2 (1010 basis functions) and BS3 (1255 basis functions). Contractions employed for all three sets of basis sets are provided in Table S1 in the Supporting Information. We have also performed calculations with two different active spaces: AS1 and AS2. In the case of AS1, the active space comprised of one active electron of Ce^{III} in the seven 4f active orbitals (RAS(1,7)). In the AS2 active space, we incorporated the $4d^{10}$ shell on top of the AS1 active space with RAS(11,12) (see Tables S2–S4 in the Supporting Information). The ground-state f-electron configuration for Ce^{III} was $4f^1$, which yielded $^2F_{5/2}$ multiplet as the ground state. CASSCF calculations were performed with the abovementioned basis sets and active spaces to determine the relative energies of the Kramers doublets (KDs) and associated *g* tensors. Herein, we computed seven triplet states in the configuration interaction (CI) procedure. After computing these spin-free excited states, we mixed all of these states by using the RASSI-SO module to compute the spin–orbit coupled states. Furthermore, we used these computed spin–orbit states in the SINGLE_ANISO program to compute the *g* tensors. To test the effect of dynamic correlations on the computed low-lying energy spectrum, we performed CASPT2 calculations on complex **2** (see the Supporting Information for details). The CASPT2 calculations yielded a similar energy pattern and associated *g* tensors to the CASSCF results. This suggested that the inclusion of a dynamic correlation did not improve the results, which was expected because lanthanide–ligand covalency was very small. The Ce^{III} ion had three low-lying KDs for which the *g* tensors were computed. For both complexes, calculations were performed on crystallographic geometries to observe the effect of charges (i.e., neighbouring molecules in the lattice) on the electronic structure, we modelled the Madelung fields by incorporating four layers of point charges (see the Supporting Information for details). The

Cholesky decomposition for two-electron integrals was employed throughout to save disk space. Using the SINGLE_ANISO code, we computed the CF parameters and constructed the ab initio blockade barrier by computing the transversal magnetic moment between each KDs to analyse the nature of magnetic relaxation.[12s]

Results and Discussions

In complex **1**, the Ce^{III} ion is nine-coordinate and is coordinated to {Zn(L)} ions on each side through two μ-phenoxo oxygen atoms and two methoxy oxygen atoms. Additionally, one methanol molecule is also ligated to the Ce^{III} ion to complete the coordination sphere. All three metal ions are aligned in a linear fashion with a Zn-Ce-Zn angle of 174°. The four phenoxo oxygen atoms occupy axial positions, while the other five oxygen donor atoms form an equatorial plane (see Figure 1 a).

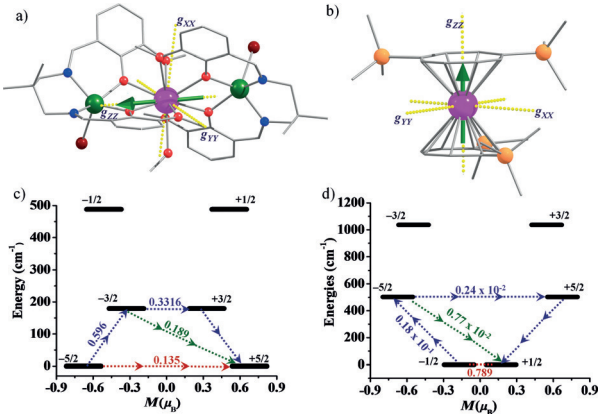

Figure 1. X-ray structures of complexes a) **1** and b) **2** showing ab initio computed orientations of the *g* tensors of the ground-state KDs. Colour code: pink, Ce; green, Zn; red oxygen; blue, nitrogen; grey wires, carbon. Hydrogen atoms are omitted for clarity. Ab initio computed magnetisation blockade barriers, along with computed transversal magnetic moments between the connecting pairs for complexes c) **1** and d) **2**.

For complex **1**, the computed ground-state anisotropies are $g_{xx}=0.331$, $g_{yy}=0.482$ and $g_{zz}=4.063$. This suggests an axial set of *g* tensors, but lacks those of a pure Ising type, which one would expect for the $m_J\,|\pm5/2\rangle$ ground state. All three KDs span an energy window of 488 cm^{-1}. The relative energies of the three low-lying KDs, along with the computed anisotropy, are given in Table 1. Wave function analysis suggests that the ground state of the Ce^{III} ion in this complex is predominantly $|\pm5/2\rangle$ ($0.78|\pm5/2\rangle-0.10|\pm3/2\rangle$) with significant mixing from the excited $|\pm3/2\rangle$ state (see Table S6 in the Supporting Information). The computed g_{zz} orientation for the ground-state KD in **1** is directed towards one of the oxygen donors of the bridging ligands and deviates from the Ce–O bond by about 11°. The g_{zz} axis is tilted by 20.8° from the Zn-Ce-Zn axis (see Figure 1 a). The first excited KD is located at about 180 cm^{-1} and possesses much larger transverse anisotropy ($g_{xx}=0.374$, $g_{yy}=1.141$, and $g_{zz}=2.564$). The first excited state is also found to be strongly mixed with consecutive excited states; this is attributed to a low-symmetry environment being present in complex **1** (see Table S6 in the Supporting Information). The principal magnetisation axis for the first excited KD is also oriented along the Zn-Ce-Zn axis, but is tilted by 36.8° from the direction of the g_{zz} axis of the ground state. The non-coincidence of the principal magnetisation axes of the ground and first excited state KD enforces magnetic relaxation to occur via the first excited KD. This suggests that the barrier height (U_{calcd}) of 180 cm^{-1} for this complex is overestimated compared with the experimentally observed barrier height (U_{eff}) of 14.7 cm^{-1}.[11a] Recently, we demonstrated the importance of dilution experiments to bridge the gap between the values of U_{eff} and U_{calcd} by an order of magnitude.[20]

Table 1. CASSCF + RASSI-SO-computed *g* tensors and relative energies of three low-lying KDs for complexes **1** and **2**, along with deviations from the principal magnetisation axes of the first KD. The values provided in parentheses are for complex **2**.

Energy [cm^{-1}]	g_{xx}	g_{yy}	g_{zz}	θ
0.0	0.331	0.483	4.063	–
(0.0)	(2.433)	(2.433)	(1.033)	
179.5	0.374	1.141	2.564	36.8
(503.1)	(0.002)	(0.011)	(4.116)	(0.98)
488.3	0.518	1.494	3.227	99.8
(1036.6)	(0.033)	(0.040)	(3.210)	(1.32)

Apart from the magnetic relaxations discussed above, another important relaxation in lanthanide SMMs is due to intermolecular interactions. To see how these intermolecular interactions influence the low-lying energy spectrum, we have modelled these interactions by using the point-charge model with the Madelung lattice constant. Herein, eight layers of point charges, four below and four above the actual molecule of interest, were considered and these point charges were constructed based on the X-ray structure and CASSCF-computed charges (see the Supporting Information for further details). Although minor changes are noted, this model also yields a similar energy spectrum with almost no change in the U_{calcd} values.

It has often been observed that extended basis sets lead to closer agreement between values of U_{calcd} and U_{eff}.[21] To test the basis-set dependence, we extended the calculations by expanding the basis set from double-ζ to triple-ζ with the active space of CAS(1,7).This leads to an increase in the value of U_{calcd} by about 10%. A similar trend has been observed when calculations have been performed by using the active space of CAS(11,12), which also incorporates the $4d^{10}$ shells (see Tables S2–S4 in the Supporting Information). The presence of larger basis sets and the active spaces did not significantly improve the values of U_{calcd} nor was an improvement to the experimental magnetic data observed (see Figure S2 in the Supporting Information). Thus, we have chosen to restrict further studies to the BS2 level basis set and CAS(1,7) active space.

To analyse magnetic relaxation in complex **1**, we constructed the ab initio magnetisation blockade barrier by computing the transverse magnetic moments between the corresponding states. Here, the states are arranged according to the values of

their magnetic moments. The number at each arrow connecting any two states is the mean absolute value of the matrix elements of the transverse magnetic moments between the corresponding states. The shortest pathway for the relaxation of magnetisation corresponds to a large value of transverse magnetic moment (see Figure 1c). This analysis suggests that the most feasible path for magnetic relaxation is that shown by the dotted blue lines in Figure 1c, that is, thermally assisted quantum tunnelling via the first excited state due to the non-coincidence of the principal g_{zz} axes of the ground-state KD and the first excited-state KD. The presence of significant transverse anisotropy ($g_{xx}=0.331$, $g_{yy}=0.483$) in the ground state due to the mixing of higher excited states suggests that the QTM will also be operative within the ground-state KD. A significant transverse magnetic moment ($0.135\,\mu_B$) within the ground-state KD and between the first excited KD suggest that both QTM and thermally assisted quantum tunnelling of magnetisation (TA-QTM) are operational and are competing processes for magnetisation relaxation. Furthermore, the off-diagonal matrix elements between the ground state and first excited-state KD ($0.18\,\mu_B$) confirm Orbach/Raman relaxation.

In complex **2**, the Ce^{III} ion is bound to two dianionic COT″ ligands in the η^8 manner with a COT″-Ce-COT″ angle of 178° (measured from the centre of the COT″ ring) and the average Ce–C(COT″) distance is 2.063 Å (see Figure 1b). The barrier height, estimated by fitting only the higher temperature data to the linear Arrhenius equation, yields $U_{eff}=30$ K for complex **2**. Because lower temperature data are non-linear, this suggests that QTM is operational for this molecule as well. We fit the data for complex **2** with Equation (1) (see Figure S7 in the Supporting Information).

$$\frac{1}{\tau}=\frac{1}{\tau_0}\exp(-\Delta E/k_BT)+\frac{1}{\tau_0^{tunnel}} \quad (1)$$

The fit yielded the following parameters: $\tau_0=1.14\times10^{-6}$ s; $\Delta E/k_B=29.5$ K and $\tau_0^{tunnel}=0.058$ s for complex **2**, and $\tau_0=1.6\times10^{-7}$ s, $\Delta E/k_B=21.2$ K and $\tau_0^{tunnel}=3.8\times10^{-4}$ s for complex **1**.[11a,b]

The computed energy spectrum for three low-lying KDs spans up to about 1036 cm^{-1} and the energies of each KD, as well the associated g tensors, are provided in Table 1. The larger energy gap (twice as big) computed for complex **2** than **1** suggests the presence of stronger metal–ligand interactions in complex **2**. The computed g tensors for the ground-state KDs are $g_{xx}=2.432$, $g_{yy}=2.361$ and $g_{zz}=1.033$; this reflect a pure rhombic set of g tensors with a small magnetic moment along the easy axis. In contrast to complex **1**, here $m_J|\pm1/2\rangle$ is the ground state (see Tables S6 and S8 in the Supporting Information). The computed static dc data also yields good agreement with the experimental data (see Figure S6 in the Supporting Information).

The computed orientation of the g_{zz} axis is collinear with the highest symmetric axis. The first excited $m_J|\pm5/2\rangle$ KD is located 503 cm^{-1} above the ground state KD and the g_{zz} of this first excited state is collinear with the ground-state KD (deviation of $<2°$). Because the ligand environment is symmetric in nature, even for the second excited KD, the g_{zz} orientation is collinear with the ground-state g_{zz} axis (see Table 1 and Table S7 and Figure S5 in the Supporting Information). This is an ideal situation of relaxation one can look for in these systems; however, a strong equatorial ligand field stabilises $m_J|\pm1/2\rangle$ as the ground state, leading to significant QTM effects. The constructed ab initio blockade barrier shows a barrier-less "U"-shaped behaviour for magnetic relaxation (see Figure 1d). Thus, no zero-field SMM behaviour is expected for this molecule. However, the application of a magnetic field lifts the degeneracy of the $m_J|\pm1/2\rangle$ levels and quenches the QTM effects to a certain extent. The hyperfine interactions, which generally open up resonant QTM behaviour in an applied field, are also absent for Ce^{III} ions because none of the natural isotopes of Ce^{III} possess any nuclear spins. This leads to an observation of magnetic relaxation for complex **2** in the presence of an applied field. If the ground-state QTM is quenched, other factors are very favourable (larger U_{calcd} values, coincidence up to the second excited state, very small QTM computed between the excited KDs, etc.) for complex **2**. This is expected to yield a larger barrier height for this molecule, as estimated from the experimental data. In addition, the value of τ_0^{tunnel} extracted from experiments is also larger for complex **2** than that of complex **1**; this is also in agreement with our calculated results.

We have also computed the CF parameters for both complexes and this provides further insights into the mechanism of magnetic relaxation. Because the CF parameters cause splitting of the ground-state multiplets and these are very sensitive to small structural changes, they offer intriguing clues to the relaxation mechanism. Recent developments in the SINGLE_ANISO code allow us to compute the CF parameters from Equation (2):

$$\hat{H}_{CF}=\sum\sum_{k=-q}^{q}B_k^q\tilde{O}_k^q \quad (2)$$

in which $\tilde{O}_k^q$ is the extended Stevens operator and B_k^q is the computed CF parameter. The computed CF parameters for complexes **1** and **2** are shown in Tables S4 and S9, respectively, in the Supporting Information.

Assuming very small or negligible intermolecular and ligand hyperfine interactions, the probability of QTM between the ground-state KD can be best described by the CF parameters. The QTM effects are expected to be dominant in a system in which the non-axial B_k^q (in which $q\neq0$ and $k=2, 4, 6$) terms are larger than the axial terms (in which $q=0$ and $k=2, 4, 6$). The computed CF parameters for complexes **1** and **2** are given Tables S4 and S9 in the Supporting Information. For complex **1**, we notice that the axial B_2^0 parameter is the largest one and it is negative. The main effect of the negative B_2^0 parameter is to stabilise the $m_J|\pm5/2\rangle$ in the ground state (Table S6 in the Supporting Information). However, quite large values of the non-axial B_2^1, B_4^1, B_4^3 terms induce significant mixing between all components of the ground $J=5/2$ manifold. As a result, the ground doublet state acquires significant transverse anisotropy ($g_{xx}=0.331$, $g_{yy}=0.483$). The presence of significant non-axial terms, alongside large values of $g_{x,y}$, suggest that the QTM at

the ground state is operative, along with TA-QTM/Orbach via the first excited KD (Figure 1 c).

On other hand, for complex **2**, in which higher symmetry around the Ce^{III} ion is maintained compared with **1**, the non-axial terms are smaller than the axial terms. We notice that the axial B_2^0 parameter is the largest one and it is positive. We also mention the opposite sign of the B_4^0 parameter relative to **1**. The main effect of the positive B_2^0 parameter is to stabilise $m_J|\pm1/2\rangle$ in the ground state (see Tables S8 and S9 in the Supporting Information). As such, the transition between the two components is significant, and induced by the first-order angular momentum operator. In other words, suppose the molecule is prepared in one of the states with a definite m_J value, any magnetic field applied along the perpendicular directions (x and y) will interact with the corresponding magnetic moments μ_x and μ_y (as reflected in the large g_x and g_y values in the ground-state KD) to induce significant Zeeman splitting, that is, quantum tunnelling. This leads to significant rates of QTM in the ground state. We may draw an analogy with the effect of the positive anisotropy parameter D in classical spin systems. Thus, the "easy-plane"-type magnetic anisotropy of the ground doublet state is not surprising. The opposite signs of the axial B_2^0 and B_4^0 parameters for **1** and **2** are associated with the dominant axial ligand field in **1** versus the dominant equatorial ligand field in **2**, and, as a result, have the inverse energy patterns of low-lying KDs. The opposite sign of the CF is a result of the axial CF in **1** versus the equatorial CF in **2**.

To gain insights into the bonding picture and how this is correlated to the ligand field and anisotropy, we performed DFT calculations on **1** and **2**, and the computed spin density plots are shown in Figure 2. Spin density analysis suggests a predominant spin polarisation mechanism for both **1** and **2**. Notably, complex **1** possess four methoxy and one methanol oxygen atoms weakly coordinated on the equatorial plane, while four negatively charged phenoxo oxygen atoms occupy the axial position. Because the Ce^{III} ion is an oblate ion, strong axial ligands are desired to stabilise larger m_J values as the ground state. The ligand arrangement in complex **1** led to stabilisation of $m_J|\pm5/2\rangle$ as the ground state. Because significant deviation in both the equatorial plane and axial directions is observed, mixing of the ground state with other excited states is expected, as exemplified by the earlier CASSCF results. DFT calculations clearly reflect this picture in which the unpaired electron of Ce^{III} is found to occupy the 4 $f_{x(x^2-3y^2)}$ orbital, leading to a disc-like spin density in the equatorial plane. Additionally, the computed (see Table S5 in the Supporting Information) charges also reveal a similar picture in which phenoxo oxygen atoms possess a significantly large negative charge compared with other oxygen donors.In contrast, for complex **2**, the COT'' ligands provide strong equatorial interactions[11b] and this leads to stabilisation of $m_J|\pm1/2\rangle$ as the ground state. DFT calculations also capture this point where the unpaired electron of Ce^{III} occupies the 4 f_{xyz} orbital, leading to a cube-shape spin density (see Figure 2 b).

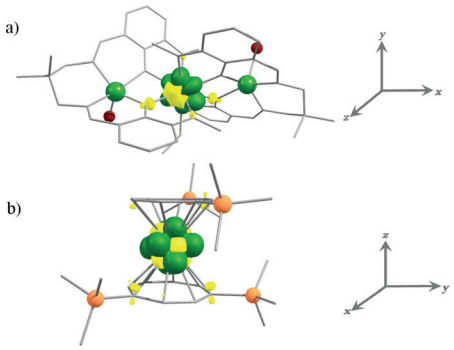

Figure 2. DFT-computed spin density plots of complexes a) **1** and b) **2**. The isodensity surface is represented with a cutoff of 0.001 e^- $bohr^{-3}$. The green and yellow regions indicate positive and negative spin densities, respectively.

Importance of geometry and C.N.s upon the U_{calcd} values: Building highly anisotropic SMMs

To answer question 4 posed earlier, we performed calculations on several fictitious model complexes of Ce^{III} with various C.N.s (1 to 12) and geometries (see Figure 3). Both symmetry and the electrostatic potential of the ligands play a vital role in dictating SMM behaviour. All model structures are generated by maintaining the closest higher order symmetry to achieve large U_{calcd} values. For this purpose, we have chosen $[Ce(OH)_n]^{m-/+}$ models, in which the Ce–O distances were fixed at 2.3 Å, the O–H distances were fixed at 1.0 Å and the Ce-O-H bond angle(s) were fixed at 180.0° to preserve the closest higher order symmetry for all of these models. The models studied herein are shown in Figure 3, and the computed g_{zz} anisotropy axis and energies of three low-lying KDs for model complexes from C.N. = 1–12 are provided in Table S10 in the Supporting Information. The following points emerge from our predictions: 1) The models for C.N. = 1 and 2 ($C_{\infty v}$ and $D_{\infty h}$) do not possess any equatorial ligation. The ground-state KD in C.N. = 1 possesses a very small transverse anisotropy, which opens up the QTM pathway and is likely to diminish the U_{eff} value. The C.N. = 2 model shows the largest U_{calcd} value among all of the models studied and can be attributed to the oblate f-electron density of the Ce^{III} ion. All KDs in the C.N. = 2 model are of pure Ising type, which causes stabilisation of $m_J|\pm5/2\rangle$ as the ground state. Moreover, all excited-state KD values of g_{zz} are collinear with the ground-state g_{zz} axis, leading to very large U_{calcd} values. 2) For models of C.N. = 3 and 4, all of the ligands are on an equatorial plane, which is an unfavourable ligand field environment for an oblate ion, and thus, these models possess significant transverse anisotropy at the ground state and stabilise $m_J|\pm1/2\rangle$ as the ground state. 3) The addition of further ligands is assumed to occur in the axial direction for C.N. = 5–7. Because addition along the axial direction is favourable for oblate ions, these models stabilise higher m_J levels as the ground state. For C.N. = 5, square-pyramidal and trigonal bipyramidal (TBP) geometries were modelled and the TBP structure was found to be superior because there were two axial ligands present in the model. 4) For C.N. = 6, significant transverse anisotropy at the ground state is noted and the computed g values resemble those of an isotropic system.

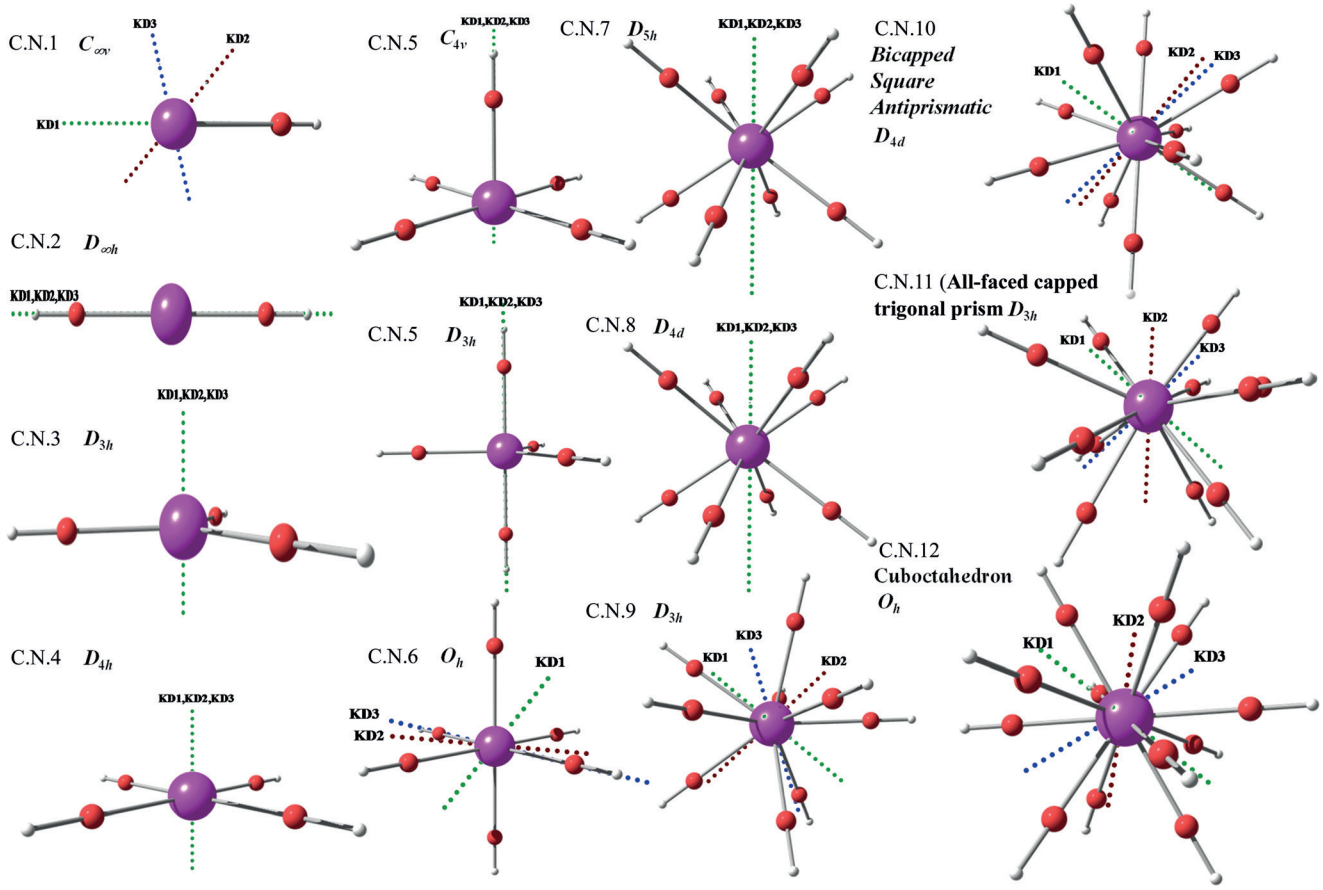

Figure 3. The ab initio computed structures along the direction of principal magnetisation axis for three low-lying KDs for models with C.N. = 1–12. Colour code: pink, Ce; red, O; white, H.

Because no unique higher order symmetry is present in the octahedral structure, the $g_{xx} \approx g_{yy} \approx g_{zz}$ situation arises. For C.N. = 7 (pentagonal bipyramidal geometry), the presence of two axial ligands and unique C_5 axis leads to a significant barrier for reorientation of magnetisation and collinearity among all g_{zz} axes. Additionally, this structure yields only a small transverse anisotropy in the ground-state KD. Together this information suggests that this model has a higher chance of SMM behaviour with the Ce^{III} ion. For complex **1**, although the C.N. of the Ce^{III} ion is nine, the structural arrangement more closely resembles that of the C.N. = 7 model. The energy pattern predicted for **1** and this model also resemble each other. This is the reason behind the zero-field SMM behaviour observed for complex **1**. Additionally, we would like to note here that, for Dy^{III} complexes, D_{5h} point-group structures are predicted to be superior to O_h point-group structures.[12r] For C.N. = 8, a square antiprismatic structure with the D_{4d} point group is assumed. Because all of the ligands are non-axial, the oblate-type density of the Ce^{III} ion faces strong repulsion from the ligand field and stabilises $m_J|\pm 1/2\rangle$ as the ground state. Due to perfect D_{4d} symmetry, the principal magnetisation axes of all three KDs are collinear, but stabilisation of $m_J|\pm 1/2\rangle$ activates the ground-state QTM as the most favourable pathway for magnetic relaxation. These $D_{4d/4h}$ geometries are unlikely to yield any zero-field SMM behaviour. Complex **2** is an illustrative example of this category, which lacks SMM behaviour due to stabilisation of $m_J|\pm 1/2\rangle$ as the ground state. A similar situation was encountered for the oblate Dy^{III} ion,[12w,z] which also lacked SMM behaviour in same ligand field; however, the prolate Er^{III} ion exhibited a record-breaking temperature of 10 K for magnetisation[22] reversal. A higher C.N., that is, greater than eight, does not offer significant improvement because the additional ligands occupy both axial and equatorial positions.

Conclusion

For the first time, we have performed ab initio calculations on two structurally diverse cerium(III)-based SMMs. Our calculations, apart from rationalising the observed magnetic properties of these two molecules, offer clues on how to enhance U_{eff} in cerium(III)-based SMMs. The conclusions derived from this work are summarised below.

Firstly, because this was the first attempt to perform CASSCF + RASSI/SINGLE_ANISO calculations on Ce^{III} SMMs, we performed a limited method assessment for which calculations with three different basis sets and two different active spaces were attempted. Larger triple-ζ basis sets do not significantly improve the computed properties. Furthermore, increasing the active space of CAS(1,7) to CAS(11,12) (at which the doubly occupied $4d^{10}$ shell is also incorporated into the active space)

also did not significantly influence the computed properties or low-lying energy spectrum. Our findings suggest that inclusion of only the 4f orbitals and 4f electron, along with a double-ζ basis set, is sufficient to describe these systems with reasonable accuracy.

Secondly, the zero-field SMM behaviour observed for complex **1** was attributed to the stabilisation of $m_J|\pm5/2\rangle$ as the ground state. The peculiarity of the structure and presence of two Zn^{II} cations at the axial positions stabilise the largest m_J level as the ground state. However, the lack of higher order symmetry around the Ce^{III} ion allows significant mixing of the ground state with excited states, leading to a large transverse anisotropy for the ground-state KD. This apparently activates the ground-state QTM effects. In addition to the ground-state QTM effects, the TA-QTM/Orbach/Raman process also leads to relaxation of magnetisation in this complex.

Thirdly, the strong equatorial field of the COT'' ligands is unfavourable for the Ce^{III} ion and this lead to stabilisation of the lowest $m_J|\pm1/2\rangle$ as the ground state, resulting in a U-shaped barrier-less energy spectrum. Although complex **2** is highly symmetric in nature and collinearity among all g_{zz} axes is maintained, the large transverse anisotropy associated with the $m_J|\pm1/2\rangle$ state leads to significant QTM behaviour at the ground state and quenches the SMM behaviour (in the absence of an applied field).

Finally, complexes **1** and **2** are ideal examples in which a suitable ligand field, but lack of symmetry is found in **1**, whereas higher symmetry, but an unsuitable ligand field, is found for complex **2**. These two contrasting examples exemplify the point that both symmetry and ligand field are important in the design of SMMs based on Ce^{III} ions. Our model studies particularly suggest that very low C.N.s or C.N. = 5/7 with TBP/PBP geometries are expected to yield larger U_{eff} values and moderate SMM behaviour.

Acknowledgements

G.R. would like to thank INSA, DST, AISRF and DST Nanomission (SR/NM/NS-1119/2011) for funding. G.R. acknowledges the IITB for access to the High-Performance Computing Facility. S.K.S. and T.G. would like to thank the CSIR and UGC for SRF positions. L.U. is a post-doctoral fellow of the Fonds Wetenschappelijk Onderzoek-Vlaanderen and also gratefully acknowledges INPAC and Methusalem Grants of KU Leuven. We would like to thank Prof. L. F. Chibotaru (Belgium) and Prof. E. Colacio (Spain) for their technical assistance.

Keywords: cerium · density functional calculations · ligand effects · magnetic properties

[1] a) T. Lis, *Acta Crystallogr. Sect. B* **1980**, *36*, 2042 – 2046; b) P. D. W. Boyd, Q. Li, J. B. Vincent, K. Folting, H. R. Chang, W. E. Streib, J. C. Huffman, G. Christou, D. N. Hendrickson, *J. Am. Chem. Soc.* **1988**, *110*, 8537 – 8539; c) A. Caneschi, D. Gatteschi, R. Sessoli, A. L. Barra, L. C. Brunel, M. Guillot, *J. Am. Chem. Soc.* **1991**, *113*, 5873 – 5874; d) R. Sessoli, D. Gatteschi, A. Caneschi, M. A. Novak, *Nature* **1993**, *365*, 141 – 143; e) R. Sessoli, H. L. Tsai, A. R. Schake, S. Y. Wang, J. B. Vincent, K. Folting, D. Gatteschi, G. Christou, D. N. Hendrickson, *J. Am. Chem. Soc.* **1993**, *115*, 1804 – 1816; f) S. M. J. Aubin, Z. Sun, L. Pardi, J. Krzystek, K. Folting, L.-C. Brunel, A. L. Rheingold, G. Christou, D. N. Hendrickson, *Inorg. Chem.* **1999**, *38*, 5329 – 5340.

[2] a) M. N. Leuenberger, D. Loss, *Nature* **2001**, *410*, 789 – 793; b) E. Saitoh, H. Miyajima, T. Yamaoka, G. Tatara, *Nature* **2004**, *432*, 203 – 206; c) M. Yamanouchi, D. Chiba, F. Matsukura, H. Ohno, *Nature* **2004**, *428*, 539 – 542; d) M. Evangelisti, F. Luis, L. J. de Jongh, M. Affronte, *J. Mater. Chem.* **2006**, *16*, 2534 – 2549; e) L. Bogani, W. Wernsdorfer, *Nat. Mater.* **2008**, *7*, 179 – 186; f) M. Manoli, A. Collins, S. Parsons, A. Candini, M. Evangelisti, E. K. Brechin, *J. Am. Chem. Soc.* **2008**, *130*, 11129 – 11139.

[3] A. Bencini, C. Benelli, A. Caneschi, R. L. Carlin, A. Dei, D. Gatteschi, *J. Am. Chem. Soc.* **1985**, *107*, 8128 – 8136.

[4] C. Benelli, A. Caneschi, D. Gatteschi, R. Sessoli, *Adv. Mater.* **1992**, *4*, 504 – 505.

[5] a) L. Charbonnière, R. Ziessel, M. Guardigli, A. Roda, N. Sabbatini, M. Cesario, *J. Am. Chem. Soc.* **2001**, *123*, 2436 – 2437; b) W. C. W. Chan, D. J. Maxwell, X. Gao, R. E. Bailey, M. Han, S. Nie, *Curr. Opin. Biotechnol.* **2002**, *13*, 40 – 46; c) J.-C. G. Bünzli, *Acc. Chem. Res.* **2006**, *39*, 53 – 61; d) M. D. Ward, *Coord. Chem. Rev.* **2007**, *251*, 1663 – 1677; e) K. Binnemans, *Chem. Rev.* **2009**, *109*, 4283 – 4374.

[6] a) J. P. André, H. R. Maecke, É. Tóth, A. A. Merbach, *J. Biol. Inorg. Chem.* **1999**, *4*, 341 – 347; b) B. Yan, Z.-d. Chen, S.-X. Wang, *Transition Met. Chem.* **2001**, *26*, 287 – 289; c) K. Binnemans, in *Handbook on the Physics and Chemistry Lanthanides of Rare-Earth, Vol. 35* (Eds.: K. A. Gschneidner, J. C. G. Bünzli, V. K. Pecharsky), Elsevier, Amsterdam, The Netherlands, **2005**, p. 107; d) S. Osa, T. Kido, N. Matsumoto, N. Re, A. Pochaba, J. Mrozinski, *J. Am. Chem. Soc.* **2004**, *126*, 420 – 421.

[7] H. L. C. Feltham, S. Brooker, *Coord. Chem. Rev.* **2014**, *276*, 1 – 33.

[8] a) N. Ishikawa, M. Sugita, T. Ishikawa, S. Koshihara, Y. Kaizu, *J. Am. Chem. Soc.* **2003**, *125*, 8694 – 8695; b) F. Pointillart, K. Bernot, R. Sessoli, D. Gatteschi, *Chem. Eur. J.* **2007**, *13*, 1602 – 1609; c) M. A. AlDamen, J. M. Clemente-Juan, E. Coronado, C. Marti-Gastaldo, A. Gaita-Arino, *J. Am. Chem. Soc.* **2008**, *130*, 8874 – 8875; d) M. A. AlDamen, S. Cardona-Serra, J. M. Clemente-Juan, E. Coronado, A. Gaita-Arino, C. Marti-Gastaldo, F. Luis, O. Montero, *Inorg. Chem.* **2009**, *48*, 3467 – 3479; e) P. H. Lin, T. J. Burchell, L. Ungur, L. F. Chibotaru, W. Wernsdorfer, M. Murugesu, *Angew. Chem. Int. Ed.* **2009**, *48*, 9489 – 9492; *Angew. Chem.* **2009**, *121*, 9653 – 9656; f) J. D. Rinehart, J. R. Long, *J. Am. Chem. Soc.* **2009**, *131*, 12558 – 12559; g) I. J. Hewitt, J. Tang, N. T. Madhu, C. E. Anson, Y. Lan, J. Luzon, M. Etienne, R. Sessoli, A. K. Powell, *Angew. Chem. Int. Ed.* **2010**, *49*, 6352 – 6356; *Angew. Chem.* **2010**, *122*, 6496 – 6500; h) G. Karotsis, S. Kennedy, S. J. Teat, C. M. Beavers, D. A. Fowler, J. J. Morales, M. Evangelisti, S. J. Dalgarno, E. K. Brechin, *J. Am. Chem. Soc.* **2010**, *132*, 12983 – 12990; i) M. A. Antunes, L. C. J. Pereira, I. C. Santos, M. Mazzanti, J. Marçalo, M. Almeida, *Inorg. Chem.* **2011**, *50*, 9915 – 9917; j) Y. Bi, Y.-N. Guo, L. Zhao, Y. Guo, S.-Y. Lin, S.-D. Jiang, J. Tang, B.-W. Wang, S. Gao, *Chem. Eur. J.* **2011**, *17*, 12476 – 12481; k) H. L. C. Feltham, F. Klöwer, S. A. Cameron, D. S. Larsen, Y. Lan, M. Tropiano, S. Faulkner, A. K. Powell, S. Brooker, *Dalton Trans.* **2011**, *40*, 11425 – 11432; l) H. L. C. Feltham, Y. Lan, F. Klöwer, L. Ungur, L. F. Chibotaru, A. K. Powell, S. Brooker, *Chem. Eur. J.* **2011**, *17*, 4362 – 4365; m) M. Gonidec, R. Biagi, V. Corradini, F. Moro, V. De Renzi, U. del Pennino, D. Summa, L. Muccioli, C. Zannoni, D. B. Amabilino, J. Veciana, *J. Am. Chem. Soc.* **2011**, *133*, 6603 – 6612; n) Y. N. Guo, G. F. Xu, Y. Guo, J. K. Tang, *Dalton Trans.* **2011**, *40*, 9953 – 9963; o) Y. N. Guo, G. F. Xu, W. Wernsdorfer, L. Ungur, Y. Guo, J. K. Tang, H. J. Zhang, L. F. Chibotaru, A. K. Powell, *J. Am. Chem. Soc.* **2011**, *133*, 11948 – 11951; p) T. Kajiwara, M. Nakano, K. Takahashi, S. Takaishi, M. Yamashita, *Chem. Eur. J.* **2011**, *17*, 196 – 205; q) T. Komeda, H. Isshiki, J. Liu, Y.-F. Zhang, N. Lorente, K. Katoh, B. K. Breedlove, M. Yamashita, *Nat. Commun.* **2011**, *2*, 217; r) S. K. Langley, L. Ungur, N. F. Chilton, B. Moubaraki, L. F. Chibotaru, K. S. Murray, *Chem. Eur. J.* **2011**, *17*, 9209 – 9218; s) P.-H. Lin, I. Korobkov, W. Wernsdorfer, L. Ungur, L. F. Chibotaru, M. Murugesu, *Eur. J. Inorg. Chem.* **2011**, *2011*, 1535 – 1539; t) J. D. Rinehart, M. Fang, W. J. Evans, J. R. Long, *J. Am. Chem. Soc.* **2011**, *133*, 14236 – 14239; u) J. D. Rinehart, M. Fang, W. J. Evans, J. R. Long, *Nat. Chem.* **2011**, *3*, 538 – 542; v) J. D. Rinehart, J. R. Long, *Chem. Sci.* **2011**, *2*, 2078 – 2085; w) A. Watanabe, A. Yamashita, M. Nakano, T. Yamamura, T. Kajiwara, *Chem. Eur. J.* **2011**, *17*, 7428 – 7432; x) A. Yamashita, A. Watanabe, S. Akine, T. Nabeshima, M. Nakano, T. Yamamura, T. Kajiwara, *Angew. Chem. Int. Ed.* **2011**, *50*, 4016 – 4019; *Angew. Chem.* **2011**, *123*, 4102 – 4105; y) M. Maeda, S. Hino, K. Ya-

mashita, Y. Kataoka, M. Nakano, T. Yamamura, T. Kajiwara, *Dalton Trans.* **2012**, *41*, 13640 – 13648.

[9] J. D. Leng, J. L. Liu, W. Q. Lin, S. Gomez-Coca, D. Aravena, E. Ruiz, M. L. Tong, *Chem. Commun.* **2013**, *49*, 9341 – 9343.

[10] a) Y. Li, X. L. Zhang, R. Qiu, Y. S. Kang, *Colloids Surf.* **2008**, *313 – 314*, 621 – 624; b) P. K. Deheri, V. Swaminathan, S. D. Bhame, Z. Liu, R. V. Ramanujan, *Chem. Mater.* **2010**, *22*, 6509 – 6517.

[11] a) S. Hino, M. Maeda, K. Yamashita, Y. Kataoka, M. Nakano, T. Yamamura, H. Nojiri, M. Kofu, O. Yamamuro, T. Kajiwara, *Dalton Trans.* **2013**, *42*, 2683 – 2686; b) J. J. Le Roy, I. Korobkov, J. E. Kim, E. J. Schelter, M. Murugesu, *Dalton Trans.* **2014**, *43*, 2737 – 2740; c) S. Hino, M. Maeda, Y. Ktaoka, M. Nakano, T. Yamamura, T. Kajiwara, *Chem. Lett.* **2013**, *42*, 1276 – 1278.

[12] a) L. Chibotaru, A. Ceulemans, H. Bolvin, *Phys. Rev. Lett.* **2008**, *101*, 033003 – 033001; b) L. F. Chibotaru, L. Ungur, A. Soncini, *Angew. Chem. Int. Ed.* **2008**, *47*, 4126 – 4129; *Angew. Chem.* **2008**, *120*, 4194 – 4197; c) B. Swerts, L. F. Chibotaru, R. Lindh, L. Seijo, Z. Barandiaran, S. Clima, K. Pierloot, M. F. A. Hendrickx, *J. Chem. Theory Comput.* **2008**, *4*, 586 – 594; d) G. Novitchi, W. Wernsdorfer, L. F. Chibotaru, J. P. Costes, C. E. Anson, A. K. Powell, *Angew. Chem. Int. Ed.* **2009**, *48*, 1614 – 1619; *Angew. Chem.* **2009**, *121*, 1642 – 1647; e) L. Ungur, W. Van den Heuvel, L. F. Chibotaru, *New J. Chem.* **2009**, *33*, 1224 – 1230; f) J. R. M. Long, F. Habib, P.-H. Lin, I. Korobkov, G. Enright, L. Ungur, W. Wernsdorfer, L. F. Chibotaru, M. Murugesu, *J. Am. Chem. Soc.* **2011**, *133*, 5319 – 5328; g) L. Ungur, L. F. Chibotaru, *Phys. Chem. Chem. Phys.* **2011**, *13*, 20086 – 20090; h) L. F. Chibotaru, L. Ungur, *J. Chem. Phys.* **2012**, *137*, 064112 – 064122; i) P. H. Guo, J. L. Liu, Z. M. Zhang, L. Ungur, L. F. Chibotaru, J. D. Leng, F. S. Guo, M. L. Tong, *Inorg. Chem.* **2012**, *51*, 1233 – 1235; j) F. Habib, J. Long, P. H. Lin, I. Korobkov, L. Ungur, W. Wernsdorfer, L. F. Chibotaru, M. Murugesu, *Chem. Sci.* **2012**, *3*, 2158 – 2164; k) S. K. Langley, N. F. Chilton, L. Ungur, B. Moubaraki, L. F. Chibotaru, K. S. Murray, *Inorg. Chem.* **2012**, *51*, 11873 – 11881; l) K. C. Mondal, A. Sundt, Y. Lan, G. E. Kostakis, O. Waldmann, L. Ungur, L. F. Chibotaru, C. E. Anson, A. K. Powell, *Angew. Chem. Int. Ed.* **2012**, *51*, 7550 – 7554; *Angew. Chem.* **2012**, *124*, 7668 – 7672; m) R. J. Blagg, L. Ungur, F. Tuna, J. Speak, P. Comar, D. Collison, W. Wernsdorfer, E. J. L. McInnes, L. F. Chibotaru, R. E. P. Winpenny, *Nat. Chem.* **2013**, *5*, 673 – 678; n) M. E. Boulon, G. Cucinotta, S. S. Liu, S. D. Jiang, L. Ungur, L. F. Chibotaru, S. Gao, R. Sessoli, *Chem. Eur. J.* **2013**, *19*, 13726 – 13731; o) S. K. Langley, D. P. Wielechowski, V. Vieru, N. F. Chilton, B. Moubaraki, B. F. Abrahams, L. F. Chibotaru, K. S. Murray, *Angew. Chem. Int. Ed.* **2013**, *52*, 12014 – 12019; *Angew. Chem.* **2013**, *125*, 12236 – 12241; p) J. J. Le Roy, M. Jeletic, S. I. Gorelsky, I. Korobkov, L. Ungur, L. F. Chibotaru, M. Murugesu, *J. Am. Chem. Soc.* **2013**, *135*, 3502 – 3510; q) J. D. Leng, J. L. Liu, Y. Z. Zheng, L. Ungur, L. F. Chibotaru, F. S. Guo, M. L. Tong, *Chem. Commun.* **2013**, *49*, 158 – 160; r) J.-L. Liu, Y.-C. Chen, Y.-Z. Zheng, W.-Q. Lin, L. Ungur, W. Wernsdorfer, L. F. Chibotaru, M.-L. Tong, *Chem. Sci.* **2013**, *4*, 3310 – 3316; s) L. Ungur, M. Thewissen, J.-P. Costes, W. Wernsdorfer, L. F. Chibotaru, *Inorg. Chem.* **2013**, *52*, 6328 – 6337; t) A. Venugopal, F. Tuna, T. P. Spaniol, L. Ungur, L. F. Chibotaru, J. Okuda, R. A. Layfield, *Chem. Commun.* **2013**, *49*, 901 – 903; u) Y.-N. Guo, L. Ungur, G. E. Granroth, A. K. Powell, C. Wu, S. E. Nagler, J. Tang, L. F. Chibotaru, D. Cui, *Sci. Rep.* **2014**, *4*, 5471; v) K. S. Pedersen, L. Ungur, M. Sigrist, A. Sundt, M. Schau-Magnussen, V. Vieru, H. Mutka, S. Rols, H. Weihe, O. Waldmann, L. F. Chibotaru, J. Bendix, J. Dreiser, *Chem. Sci.* **2014**, *5*, 1650 – 1660; w) L. Ungur, J. J. Le Roy, I. Korobkov, M. Murugesu, L. F. Chibotaru, *Angew. Chem. Int. Ed.* **2014**, *53*, 4413 – 4417; *Angew. Chem.* **2014**, *126*, 4502 – 4506; x) T. Gupta, G. Rajaraman, *J. Chem. Sci.* **2014**, *126*, 1569 – 1579; y) S. K. Singh, T. Gupta, M. Shanmugam, G. Rajaraman, *Chem. Commun.* **2014**, *50*, 15513 – 15516; z) S. K. Singh, T. Gupta, G. Rajaraman, *Inorg. Chem.* **2014**, *53*, 10835 – 10845; aa) A. Upadhyay, S. K. Singh, C. Das, R. Mondol, S. K. Langley, K. S. Murray, G. Rajaraman, M. Shanmugam, *Chem. Commun.* **2014**, *50*, 8838 – 8841.

[13] P. A. Malmqvist, B. O. Roos, B. Schimmelpfennig, *Chem. Phys. Lett.* **2002**, *357*, 230 – 240.

[14] a) G. Karlström, R. Lindh, P. A. Malmqvist, B. O. Roos, U. Ryde, V. Veryazov, P. O. Widmark, M. Cossi, B. Schimmelpfennig, P. Neogrady, L. Seijo, *Comput. Mater. Sci.* **2003**, *28*, 222 – 239; b) V. Veryazov, P. O. Widmark, L. Serrano-Andres, R. Lindh, B. O. Roos, *Int. J. Quantum Chem.* **2004**, *100*, 626 – 635; c) J. A. Duncan, *J. Am. Chem. Soc.* **2009**, *131*, 2416 – 2416; d) F. Aquilante, L. De Vico, N. Ferre, G. Ghigo, P. A. Malmqvist, P. Neogrady, T. B. Pedersen, M. Pitonak, M. Reiher, B. O. Roos, L. Serrano-Andres, M. Urban, V. Veryazov, R. Lindh, *J. Comput. Chem.* **2010**, *31*, 224 – 247.

[15] a) C. J. Milios, R. Inglis, A. Vinslava, R. Bagai, W. Wernsdorfer, S. Parsons, S. P. Perlepes, G. Christou, E. K. Brechin, *J. Am. Chem. Soc.* **2007**, *129*, 12505 – 12511; b) K. Bernot, J. Luzon, L. Bogani, M. Etienne, C. Sangregorio, M. Shanmugam, A. Caneschi, R. Sessoli, D. Gatteschi, *J. Am. Chem. Soc.* **2009**, *131*, 5573 – 5579.

[16] J.-P. Costes, J.-P. Laussac, F. Nicodeme, *J. Chem. Soc. Dalton Trans.* **2002**, 2731 – 2736.

[17] a) I. Oyarzabal, J. Ruiz, J. M. Seco, M. Evangelisti, A. Camón, E. Ruiz, D. Aravena, E. Colacio, *Chem. Eur. J.* **2014**, *20*, 14262 – 14269; b) J. Ruiz, G. Lorusso, M. Evangelisti, E. K. Brechin, S. J. A. Pope, E. Colacio, *Inorg. Chem.* **2014**, *53*, 3586 – 3594.

[18] F. Pointillart, K. Bernot, S. Golhen, B. Le Guennic, T. Guizouarn, L. Ouahab, O. Cador, *Angew. Chem. Int. Ed.* **2015**, *54*, 1371 – 1371; *Angew. Chem.* **2015**, *127*, 1389 – 1389.

[19] B. O. Roos, R. Lindh, P. A. Malmqvist, V. Veryazov, P. O. Widmark, A. C. Borin, *J. Phys. Chem. A* **2008**, *112*, 11431 – 11435.

[20] C. Das, A. Upadhyay, S. Vaidya, S. K. Singh, G. Rajaraman, M. Shanmugam, *Chem. Commun.* **2015**, *51*, 6137 – 6140.

[21] R. Marx, F. Moro, M. Dorfel, L. Ungur, M. Waters, S. D. Jiang, M. Orlita, J. Taylor, W. Frey, L. F. Chibotaru, J. van Slageren, *Chem. Sci.* **2014**, *5*, 3287 – 3293.

[22] K. R. Meihaus, J. R. Long, *J. Am. Chem. Soc.* **2013**, *135*, 17952 – 17957.

Received: April 4, 2015
Published online on August 11, 2015